Electronic Supplementary Material (ESI) for Journal of Materials Chemistry C.

SUPPORTING INFORMATION

An air-stable n-type bay-and-headland substituted bis-cyano N-H functionalized perylene diimide for printed electronics

Irene E. Park, Samantha Brixi, Mark Martell, Michael U. Ocheje, Richard D. Pettipas, Dylan H. Harris, Benjamin S. Gelfand, Simon Rondeau-Gagné, Benoit H. Lessard, and Gregory C. Welch*

Department of Chemistry, University of Calgary, 2500 University Drive N.W., Calgary, Alberta, T2N 1N4, Canada. E-mail: *gregory.welch@ucalgary.ca

Department of Chemical and Biological Engineering, University of Ottawa, 161 Louis Pasteur, Ottawa, Ontario, K1N 6N5, Canada.

Department of Chemistry and Biochemistry, Advanced Materials Centre of Research (AMCORe), University of Windsor, Ontario, N98 3P4, Canada

TABLE OF CONTENTS

1. Materials and Methods

Materials: All reagents and solvents were purchased from Millipore-Sigma and used without further purification. *N*,*N*-dimethylacetamide solvent was dried by storing over 3 Å molecular sieves and purged with N_2 gas before use. **X1** was synthesized as previously reported.[1]

Nuclear Magnetic Resonance (NMR): ^{1}H, ^{13}C and 2D NMR spectroscopy experiments were recorded using a Bruker Avance III 400 MHz or Bruker Avance III 600 MHz spectrometer at 300 K. All experiments were performed in chloroform-d (CDCl3).

High-resolution Mass Spectrometry (HRMS): High-resolution MALDI mass spectrometry measurements were performed courtesy of Johnson Li in the Chemical Instrumentation Facility at the University of Calgary. A Bruker Autoflex III Smartbeam MALDI-TOF (Na:YAG laser, 355nm), setting in positive reflective mode, was used to acquire spectra.

CHN Elemental Analysis: Elemental analyses were performed by Johnson Li in the Chemical Instrumentation Facility at the University of Calgary. A Perkin Elmer 2400 Series II CHN Elemental Analyzer was used to obtain CHN data, using ~1.5 mg of sample (with particle sizes ranging between 0.2 and 0.5 mm in diameter).

UV-Visible Spectroscopy (UV-Vis): Optical absorption measurements were performed using Agilent Technologies Cary 60 UV-Vis spectrometer at room temperature. All solution experiments were run in $CHCl_3$ using 2 mm quartz cuvettes. Films were spin-cast from 40 uL of 5 mg/mL solution of **X6** onto Corning glass micro slides that were cleaned with acetone and isopropanol, followed by UV/ozone treatment using a Novascan UV/ozone cleaning system.

Cyclic Voltammetry (CV): Electrochemical measurements were performed using a CH Instruments Inc. Model 1200B Series Handheld Potentiostat. A standard 3-electrode setup was utilized, consisting of a freshly polished glassy carbon disk working electrode (WE), Pt-wire counter electrode (CE), and Ag-wire pseudo-reference electrode (RE). All measurements were referenced to ferrocene (Fc+/0) as internal standard. All cyclic voltammetry experiments were performed at a scan rate of 100 mV/s. Sample solutions, with 1 mM compound and 0.1 M tetrabutylammonium hexafluorophosphate (TBAPF6) supporting electrolyte, were prepared in anhydrous dichloromethane. All electrochemical solutions were sparged with dry gas (either N2 or argon) for 5 minutes to deoxygenate the system prior to measurements.

Density Functional Theory (DFT) and pKa Calculation: The DFT and pKa calculations were done by Michael Ocheje from the University of Windsor. DFT calculations were performed with the dispersion corrected B3LYP-D3 functional and the 6-31G(d,p) basis set in Gaussian 09.[2] All structures were first optimized at the B3LYP-D3/6-31 G(d,p) level of theory to achieve the ground-state equilibrium geometry, which was then confirmed through frequency analysis. The gas phase calculations were performed using the B3LYP-D3 functional and the 6-31G(d,p) basis set in Gaussian 09. The SMD implicit solvation model was used to calculate the energies of solvation in DMSO solvent.[3] Both calculations were then used to calculate the deprotonation free energies and

the pKas of the three derivatives as in cycle 1.[4] A proton solvation free energy of -1143.5 kJ/mol was used in equation 2 ($\Delta G^*_s(H^+)$) to calculate the pKa.

1) $\Delta G^*_s = G_{solution} - G_{gas}$
2) $\Delta G^*_{solution} = \Delta G^*_{gas} + \Delta G^*_s(H^+) + \Delta G^*_s(A^-) - \Delta G^*_s(HA)$
3) $pK_a(HA) = \frac{\Delta G^* soln}{RTln(10)}$

TD-DFT calculations were also performed to determine the singlet excited states of X1 and X6. The calculated vertical transition energies (eV), wavelengths (nm), oscillator strengths (f) and dominant electronic configuration for the $S_0 \rightarrow S_{1\text{-}15}$ excitations are summarized in Table S3.

Single Crystal XRD: SC-XRD was done by Ben Gelfand from the University of Calgary. Single crystals of $C_{47}H_{37}Br_2N_3O_4$, **Br_2-X1**, were grown by diffusion of acetonitrile (1 mL) into a tetrahydrofuran (1 mL) solution at 298K. A suitable crystal was selected and mounted on a glass loop using Paratone. Diffraction experiments were performed on a Bruker Smart diffractometer equipped with an Incoatec Microfocus (Cu Kα, λ = 1.54178 Å) and an APEX II CCD detector. The crystal was kept at 173 K during data collection. Diffractions spots were integrated and scaled with SAINT,[5] and the space group was determined with XPREP.[6] Using Olex2,[7] the structure was solved with the ShelXT,[8] structure solution program using Intrinsic Phasing and refined with the ShelXL,[9] refinement package using Least Squares minimisation. Electron density contributions from unidentified diffuse solvent molecules were modelled using the SQUEEZE routine in PLATON.[10] CCDC # 2103127.

OFET Device Fabrication: Substrates were prepared using Fraunhofer IPMS OFET Gen5 OFET structures with an Si gate, SiO2 (230 nm thickness) dielectric, and gold source/drain contacts. Substrates were rinsed with acetone to remove photoresist, then plasma-treated for 10 minutes to clean the surface and activate the surface hydroxyl groups. The structures were then submerged in solutions of 1% octyltrichlorosilane in toluene (v/v) for 10 minutes to passivate the surface. OFET devices were fabricated *via* spin-casting in a nitrogen glovebox. 10 mg/mL solutions of X6 in $CHCl_3$ and 2Me-THF were prepared and deposited on substrates at 4k rpm for 60 seconds. N2200 was dissolved in o-dichlorobenzene at 10mg/mL, with the same deposition conditions. Devices were then thermally annealed at either 70 or 150 °C under vacuum to remove residual solvent. Channel length = 2.5 micron.

2. Synthetic Procedure

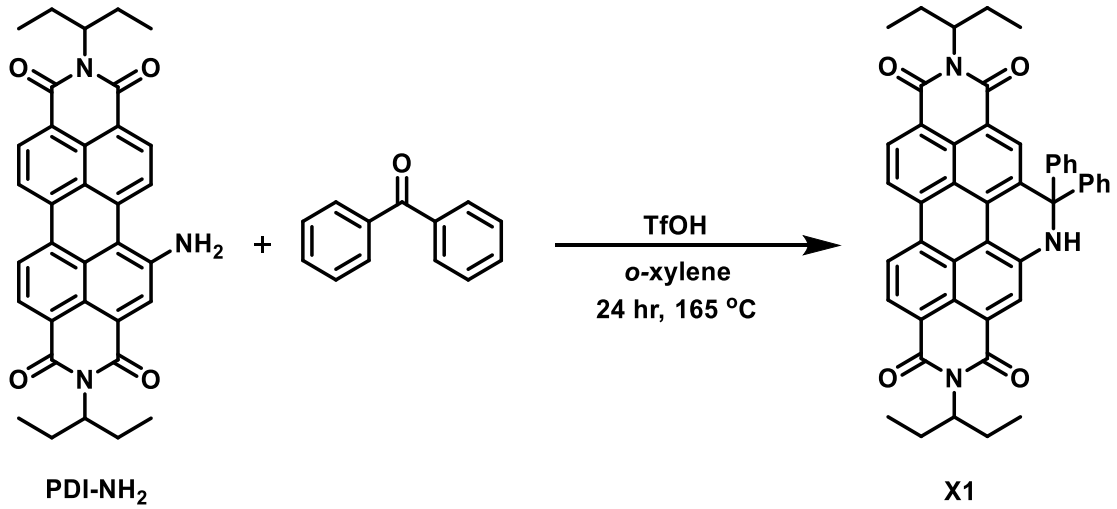

^{1}H-NMR data for this compound matches the literature.[1]

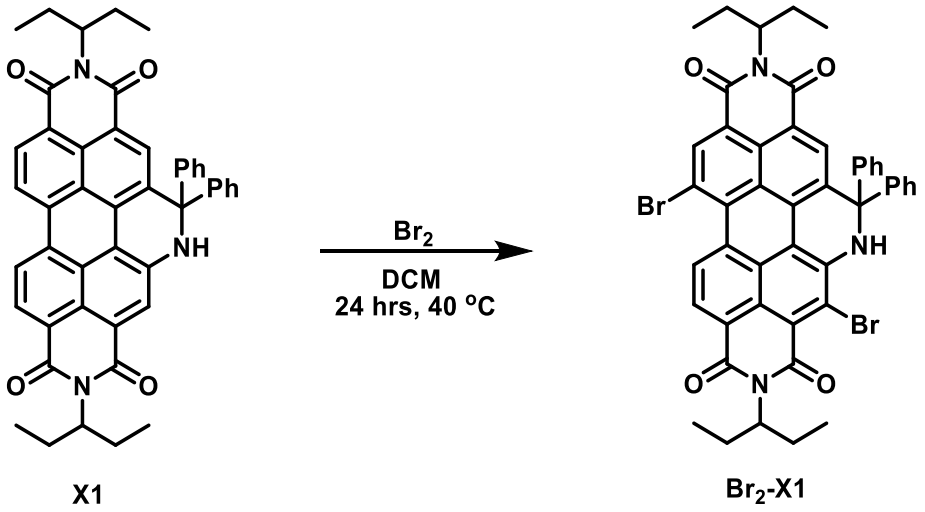

To a 20 mL pressure vial equipped with a stir bar, **X1** (126 mg, 0.177 mmol, 1.0 eq.) and 15 mL of dichloromethane (DCM) were added. To this mixture was added ~2 mL of the bromine stock solution (1.3 M, 2.6 mmol, 14 eq.), which was prepared by adding 0.2 mL of liquid bromine into 3 mL of DCM. The pressure vial was capped and stirred at 40 °C for 24 hours. Then, excess bromine in the reaction mixture was fully quenched with saturated $Na_2S_2O_5$ aqueous solution. The reaction mixture was poured into a 250 mL separatory funnel and diluted with DCM. The organic layer was washed with water twice. The collected organic layer was dried with $MgSO_4$, then vacuum filtered into a 250 mL round bottom flask. The solvent was removed *in vacuo*. The resulting crude was redissolved in DCM and loaded on silica and was subjected to silica gel column chromatography using toluene (1% ethyl acetate) as eluent. The first green-band fraction was

collected, and the solvent was removed *in vacuo*. The resulting solid was slurried in MeOH and the solid flakes collected *via* vacuum filtration to obtain pure **Br_2-X1** as a black solid (131 mg, 85%).

MALDI: Calculated (M-2H)+H^+ for $C_{47}H_{37}Br_2N_3O_4$: 864.1067; detected (M-2H)+H^+: 864.1078.

^{1}H NMR (400 MHz, $CDCl_3$): δ 9.95 ppm (d, *J* = 8.4 Hz, 1H, H_a), 8.97 (s, 1H, H_b), 8.55 (d, *J* = 8.4 Hz, 1H, H_c), 8.12 (s, 1H, H_d), 7.41 – 7.31 (m, 10H, H_e), 6.84 (s, 1H, H_f), 5.12 – 5.04 (m, 2H, H_g), 2.31 – 2.18 (m, 4H, H_h), 2.02 – 1.89 (m, 4H, H_h), 0.93 (q, 12H, H_i).

^{13}C NMR (150 MHz, $CDCl_3$): δ 163.65 ppm (1), 144.76 (2), 140.05 (3), 134.41 (4), 132.73, 131.32, 128.74 (5), 128.63 (6), 128.52 (7), 128.27, 127.73, 127.55, 127.20, 125.83, 124.02, 123.14, 122.39, 119.77, 113.79, 69.03 (8), 58.42 (9), 58.03 (9), 25.17 (10), 25.13 (10), 11.54 (11), 11.53 (11)

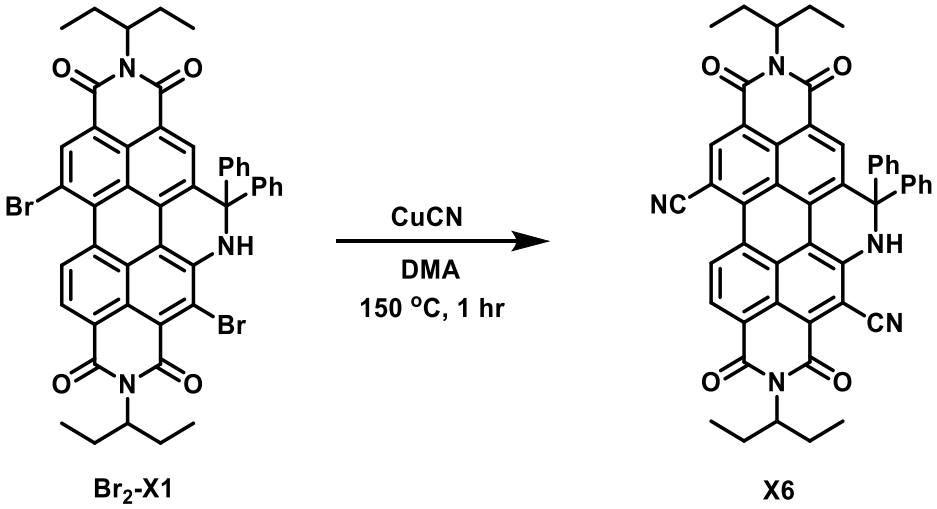

Br_2-X1 X6

To a 20 mL pressure vial equipped with a stir bar, **Br_2-X1** (159.4 mg, 0.184 mmol, 1.0 eq.) and CuCN (662.9 mg, 7.40 mmol, 40 eq.) were added. The vial was capped under N_2. Then, 5 mL of anhydrous, degassed *N,N*-dimethylacetamide (DMA) was added *via* cannula transfer to the reaction vial. The reaction was heated to 150 °C. When TLC (DCM eluent) showed no starting material with a single green spot, the reaction mixture was cooled to room temperature. The reaction mixture changed from a dark green to brighter green colour. The reaction mixture was poured into a 250 mL separatory funnel and diluted with DCM. The organic layer was washed three times with saturated NH_4Cl aqueous solution to remove excess CuCN. The organic layer was collected, dried with $MgSO_4$ and filtered through a silica plug into a 250 mL round bottom flask. The solvent was removed *in vacuo*. The resulting solid was slurried in water:methanol (1:1 v/v) and the solid flakes collected *via* vacuum filtration to obtain pure **X6** as a green solid (118.5 mg, 85%).

MALDI: Calculated M+Na^+ for $C_{49}H_{37}N_5O_4$: 782.2738; detected M+Na^+: 782.2753

^{1}H NMR (400 MHz, $CDCl_3$): δ 9.94 ppm (d, *J* = 8.3 Hz, 1H, H_a), 8.92 (s, 1H, H_b), 8.62 (d, *J* = 8.3 Hz, 1H, H_c), 8.22 (s, 1H, H_d), 7.44 – 7.37 (m, 6H, H_e), 7.32 – 7.29 (m, 4H, H_f), 6.56 (s, 1H, H_g), 5.10 – 5.02 (m, 2H, H_h), 2.30 – 2.17 (m, 4H, H_i), 2.03 – 1.90 (m, 4H, H_i), 0.93 (q, 12 H, H_j)

^{13}C NMR (100 MHz, $CDCl_3$): δ 162.00 ppm (1), 144.37 (2), 143.12, 137.63, 137.15 (3), 133.70 (4), 133.15, 130.15, 129.98, 129.96 (5), 129.24 (6), 129.05 (7), 128.91 (8), 128.54 (9), 128.33, 127.13, 125.88, 125.39, 122.38, 120.00, 115.40, 113.58, 106.51, 102.37, 68.88 (10), 58.81(11), 58.35 (11), 25.04 (12), 24.98 (12), 11.52 (13), 11.45 (13)

CHN: Theoretical (%) C: 77.45, H: 4.91, N: 9.22; found (%) C: 76.31, H: 4.83, N: 9.23

3. ^{1}H NMR Spectroscopy

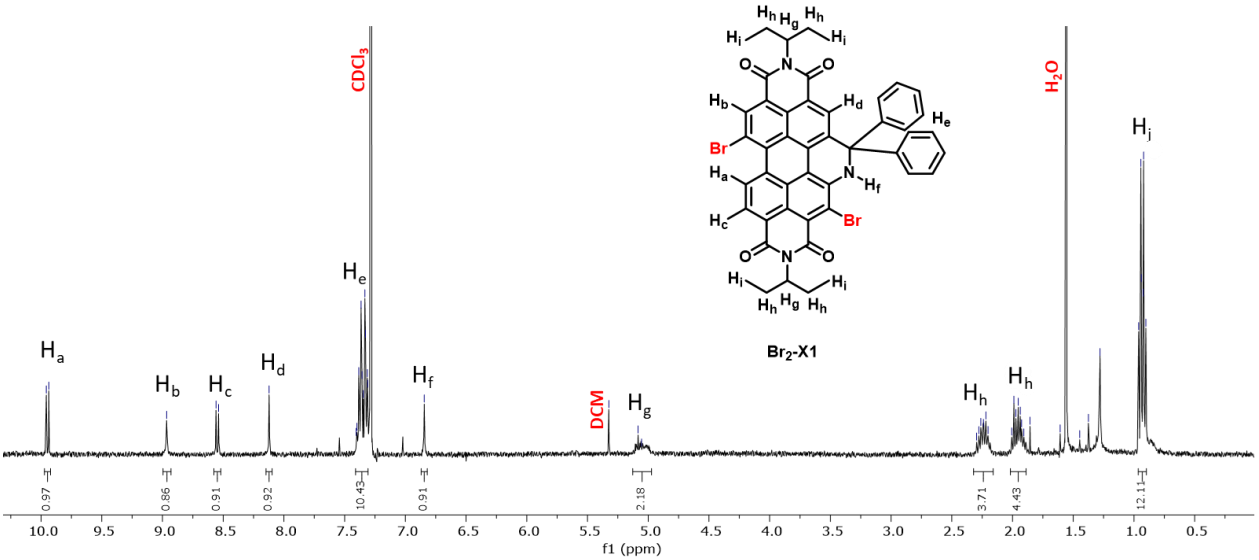

Figure S1. ^{1}H NMR spectrum of **Br_2-X1** (400 MHz, $CDCl_3$).

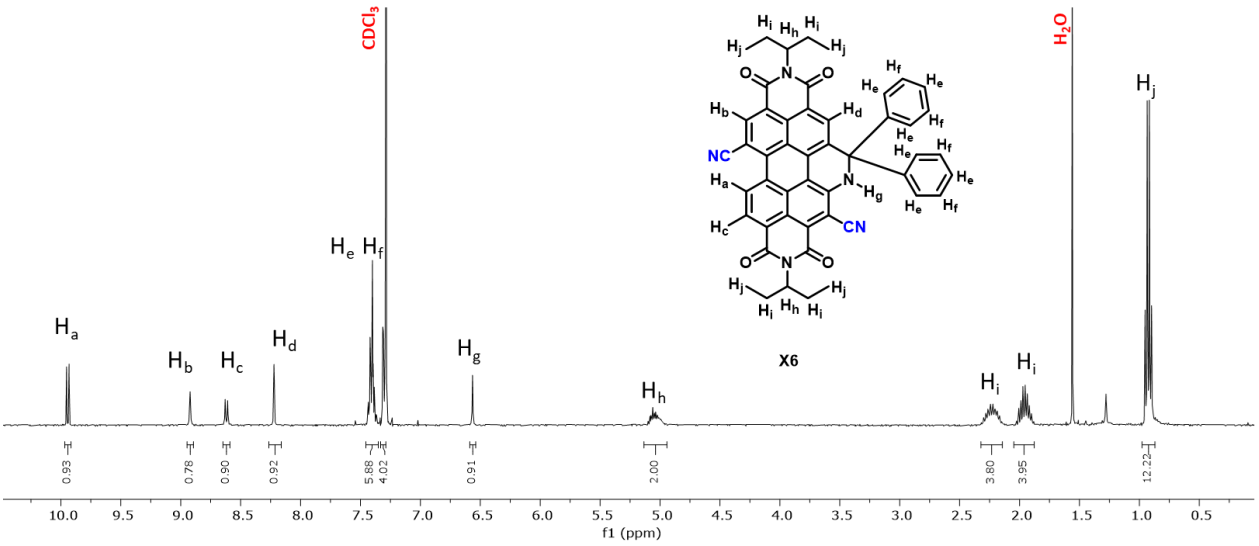

Figure S2. ^{1}H NMR spectrum of **X6** (400 MHz, $CDCl_3$).

4. ^{13}C NMR Spectroscopy

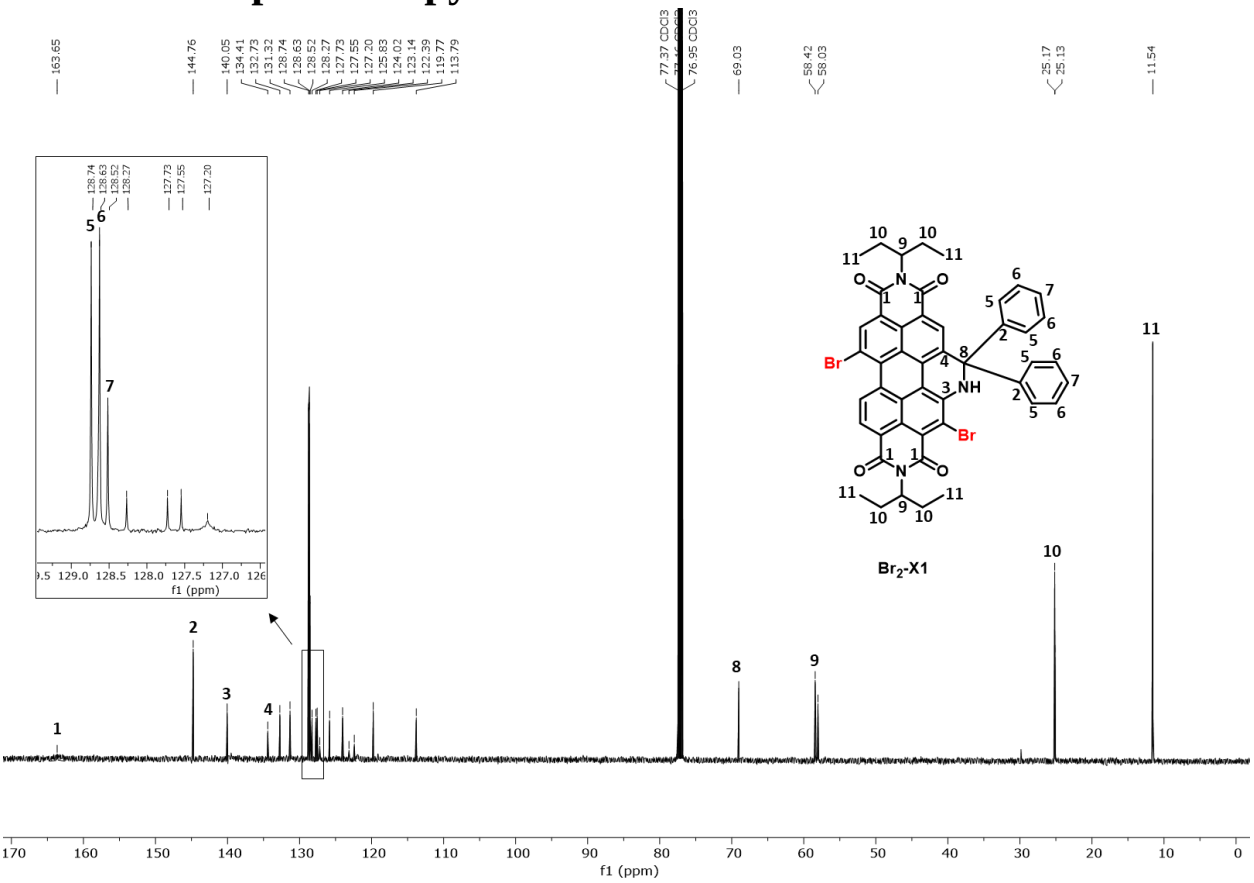

Figure S3. ^{13}C NMR spectrum of **Br2-X1** (150 MHz, $CDCl_3$).

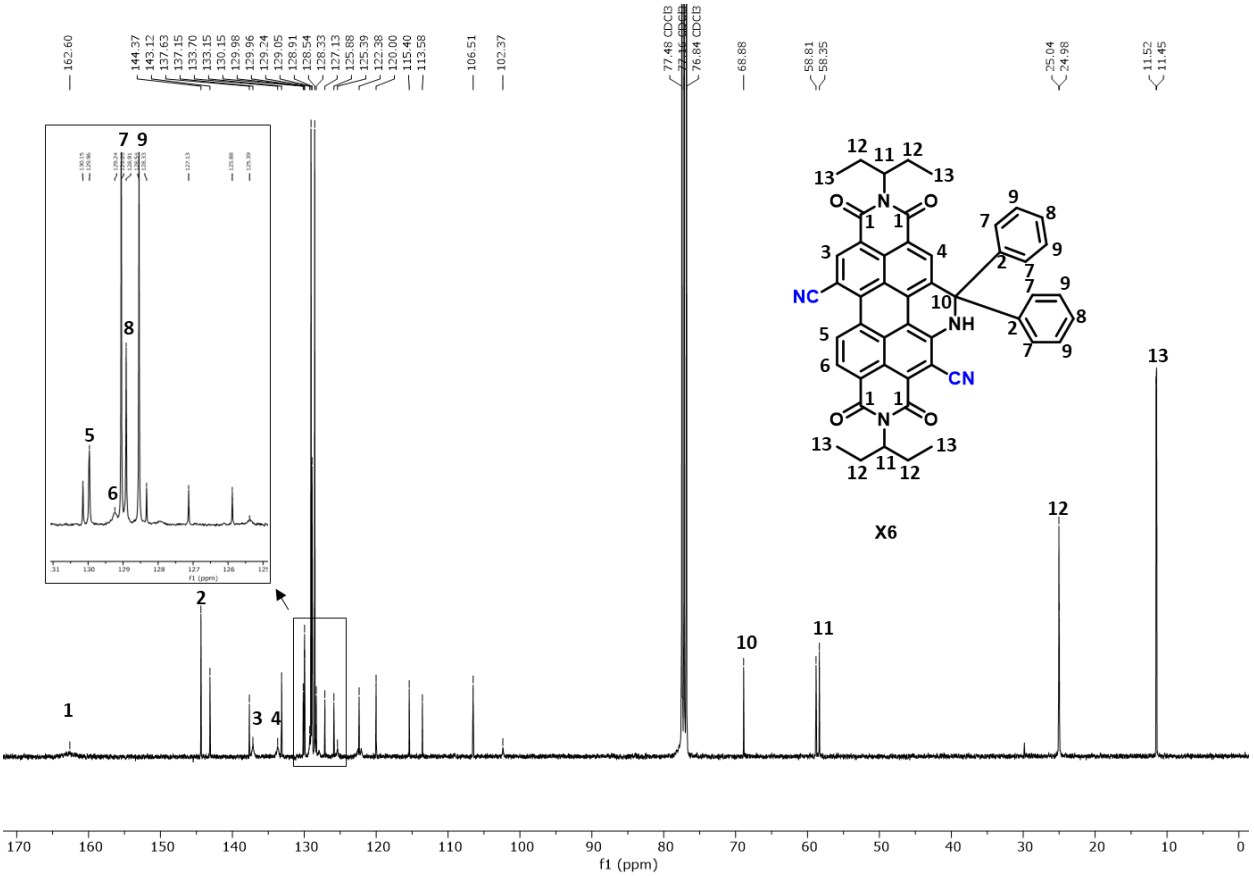

Figure S4. ^{13}C NMR spectrum of **X6** (100 MHz, $CDCl_3$).

5. 2D NMR Spectroscopy

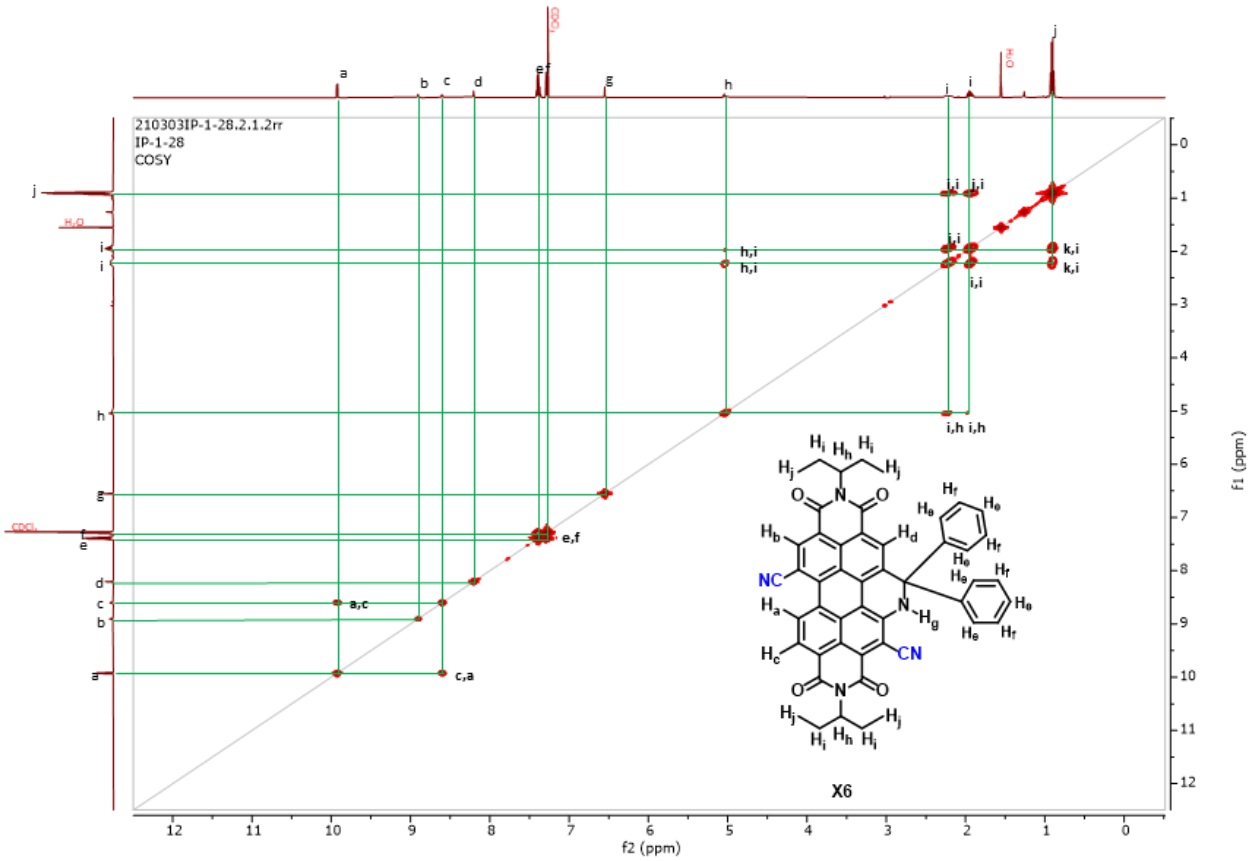

Figure S5. 2D correlation spectroscopy (COSY) spectrum of **X6** (400 MHz, $CDCl_3$).

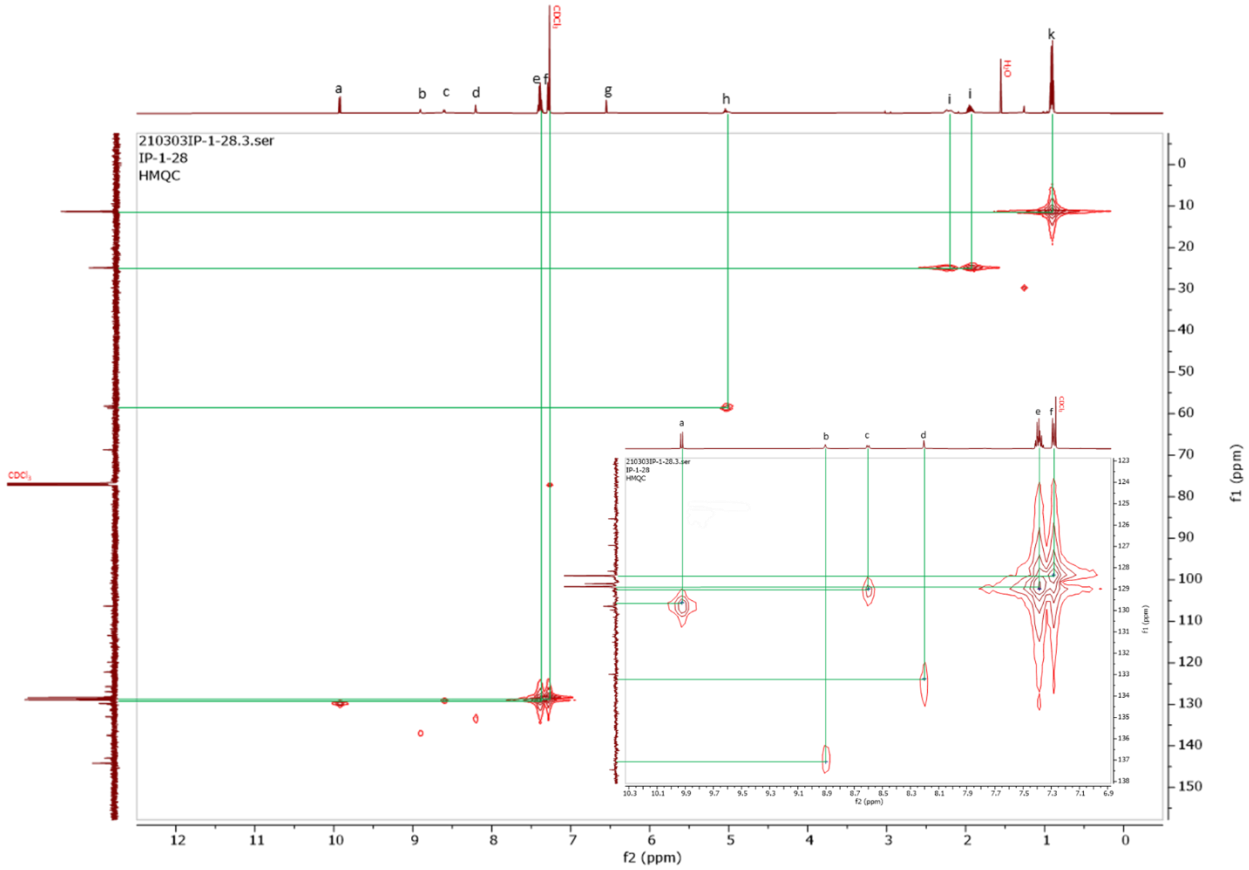

Figure S6. Heteronuclear multiple quantum coherence (HMQC) spectrum of **X6**.

6. MALDI Mass Spectrometry

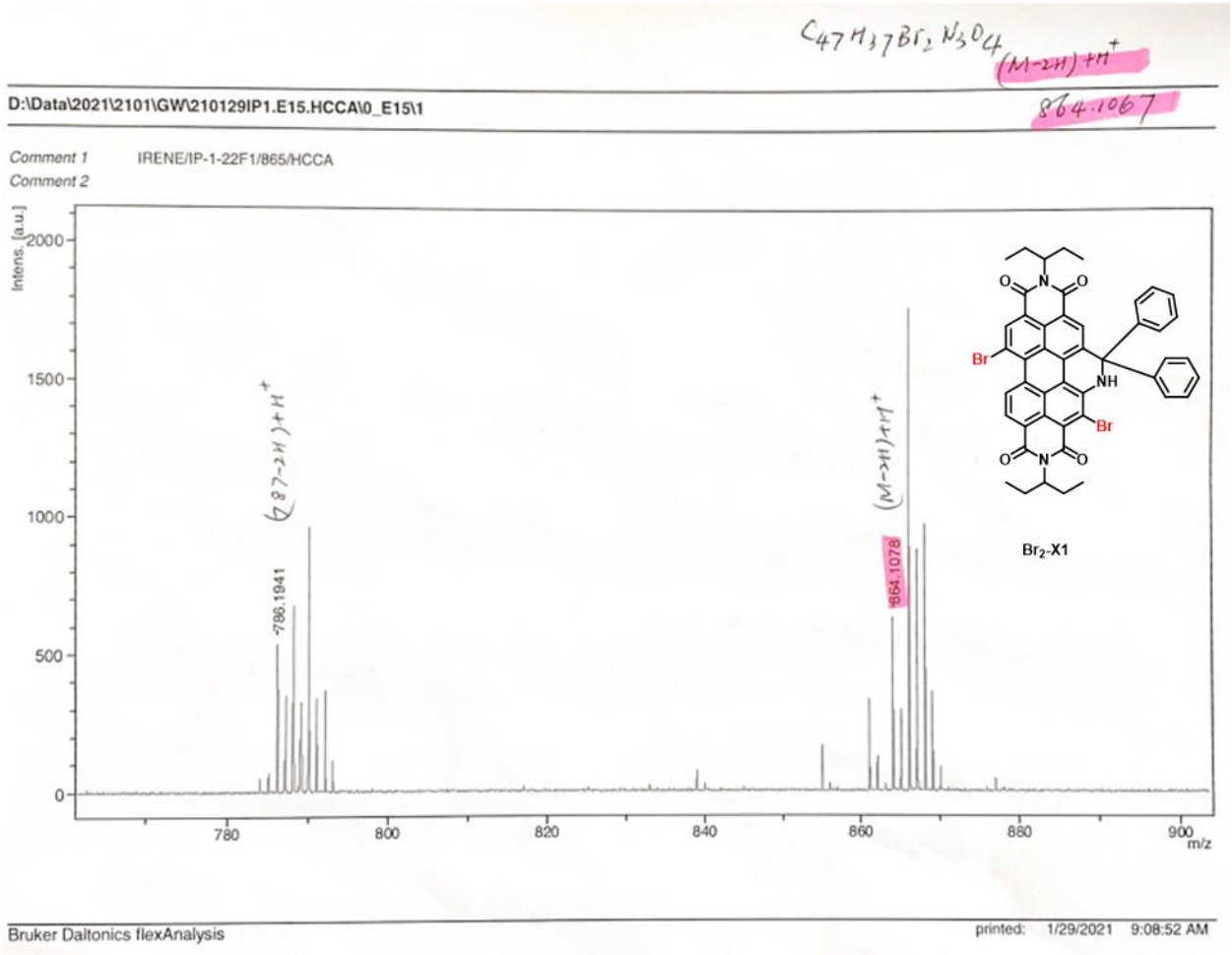

Figure S7. MALDI mass spectrometry of **Br_2-X1**: Calculated $(M-2H)+H^+$ for $C_{47}H_{37}Br_2N_3O_4$: 864.1067; detected $(M-2H)+H^+$: 864.1078.

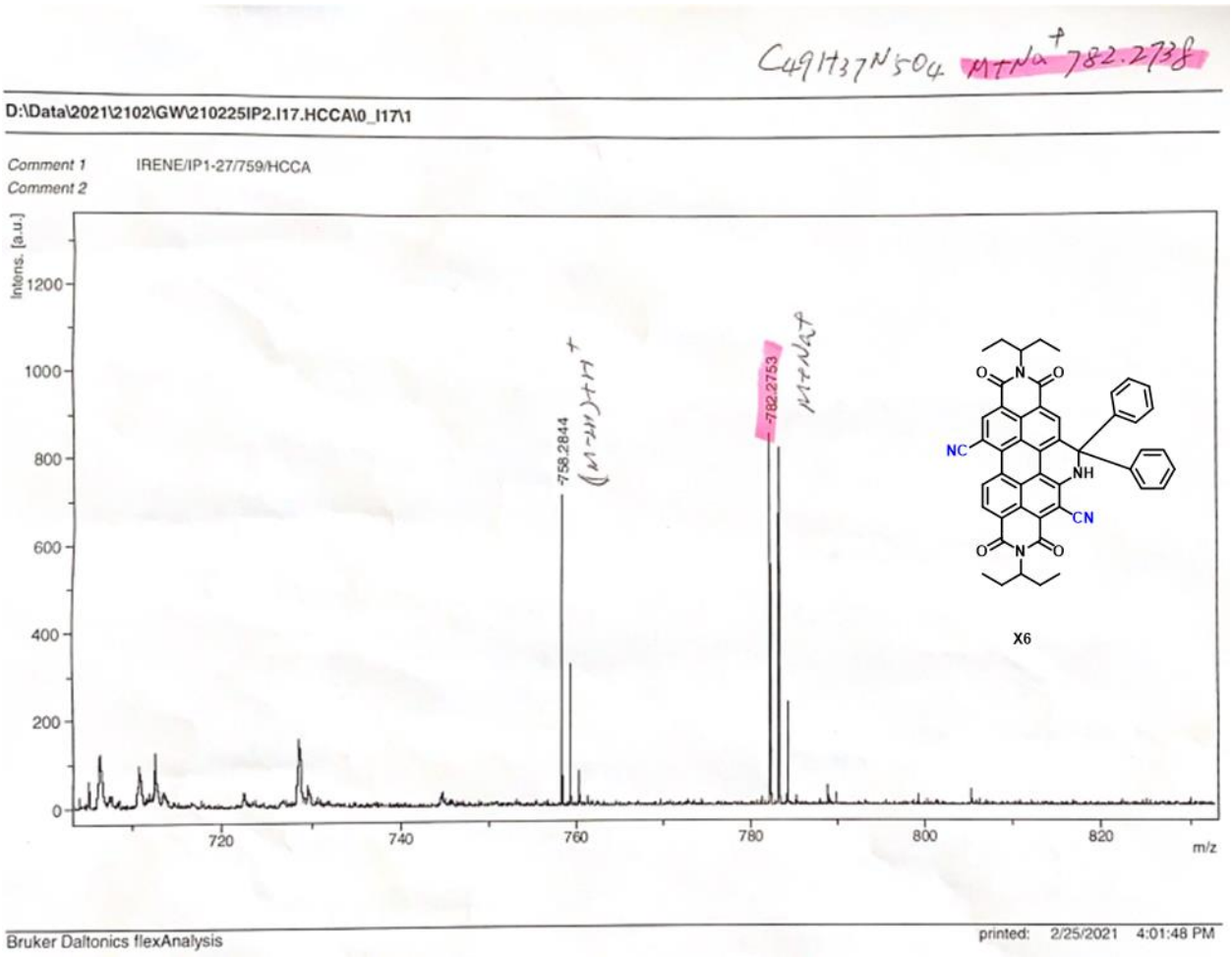

Figure S8. MALDI mass spectrometry of **X6**: Calculated M+Na^+ for $C_{49}H_{37}N_5O_4$: 782.2738; detected M+Na^+: 782.2753.

7. Elemental Analysis

University of Calgary
Department of Chemistry EA Date: 3-10-2021

Name:	IRENE	Group:	GW
Sample:	IP1-28-2	Weight (mg):	1.298
%C (Actual):	76.31	%C (Theorectical):	77.45
%H (Actual):	4.83	%H (Theoretical):	4.91
%N (Actual):	9.23	%N (Theoretical):	9.22

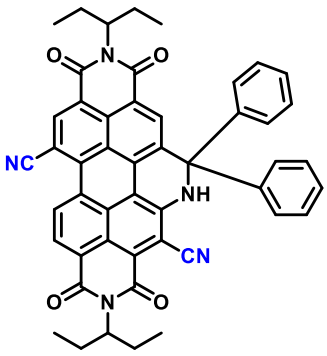

X6

Figure S9. CHN elemental analysis of **X6**.

8. SC-XRD

Table S1. Crystal data and structure refinement for **Br_2-X1**. CCDC # 2103127.

Identification code	**Br_2-X1**
Empirical formula	$C_{47}H_{37}Br_2N_3O_4$
Formula weight	867.61
Temperature/K	173
Crystal system	triclinic
Space group	P-1
a/Å	10.4795(6)
b/Å	11.5360(6)
c/Å	16.9033(9)
α/°	106.125(3)
β/°	105.399(4)
γ/°	97.187(3)
Volume/Å^3	1848.46(18)
Z	2
ρ_{calc}g/cm^3	1.559
μ/mm^{-1}	3.201
F(000)	884.0
Crystal size/mm^3	0.232 × 0.124 × 0.049
Radiation	CuKα (λ = 1.54178)
2Θ range for data collection/°	5.734 to 133.154
Index ranges	$-12 \leq h \leq 12$, $-13 \leq k \leq 13$, $-20 \leq l \leq 20$
Reflections collected	19031
Independent reflections	6288 [R_{int} = 0.0457, R_{sigma} = 0.0563]
Data/restraints/parameters	6288/142/553
Goodness-of-fit on F^2	1.040
Final R indexes [I>=2σ (I)]	R_1 = 0.0421, wR_2 = 0.1120
Final R indexes [all data]	R_1 = 0.0533, wR_2 = 0.1200
Largest diff. peak/hole / e Å^{-3}	0.87/-0.54

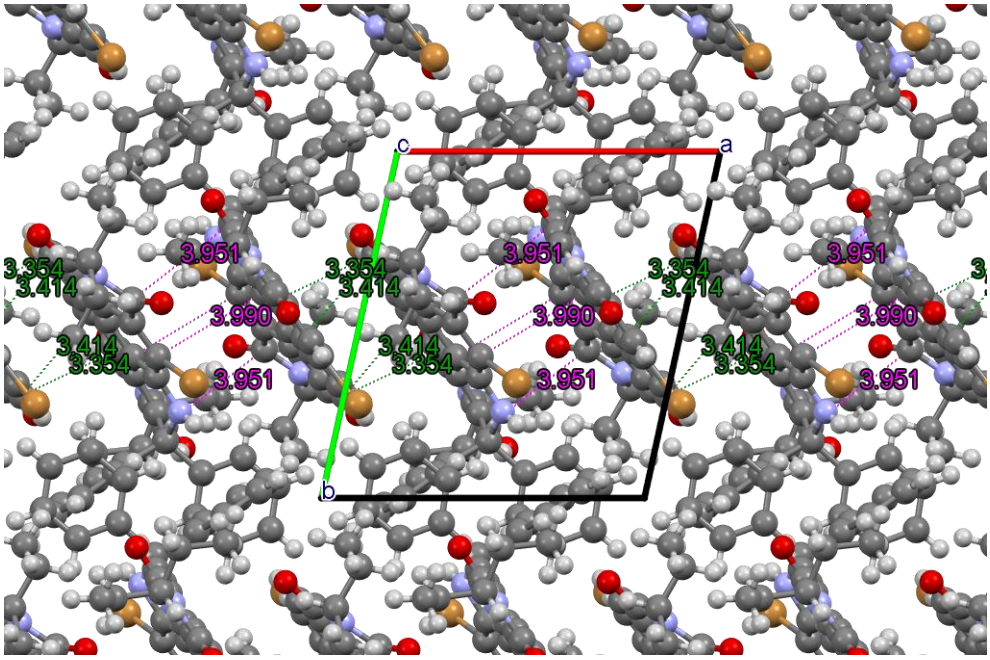

Figure S10. SC-XRD of **Br_2-X1** viewed along the c-axis, showing stacking relationships with intermolecular separation distance (Å). C, N, O, H and Br are denoted as grey, blue, red, white, and orange spheres, respectively.

9. Electrochemical Analysis

Table S2. Electrochemical data for **X1**, **X6** and **PDI**

	Ox E_{on} (V)	Ox $E_{1/2}$ (V)	Red E_{on} (V)	Red $E_{1/2}$ (V)	IP (eV)	EA (eV)
X6	0.89	1.00	-0.65	-0.74, -1.07	5.7	4.2
Br_2-X1	0.74	0.83	-0.94	-1.05, -1.26	5.5	3.9
X1[1]	0.5	0.62	-1.1	-1.22, -1.43	5.3	3.7
PDI[1]	N/A	N/A	-1.0	-1.14, -1.36	N/A	3.8

Ox E_{on} = oxidation onset
Ox $E_{1/2}$ = oxidation half potential
Red E_{on} = reduction onset
Red $E_{1/2}$ = reduction half potential
IP = ionization potential (Ox E_{on} + 4.8 eV) where Fc HOMO = 4.8 eV
EA = electron affinity (Red E_{on} + 4.8 eV) where Fc HOMO = 4.8 eV

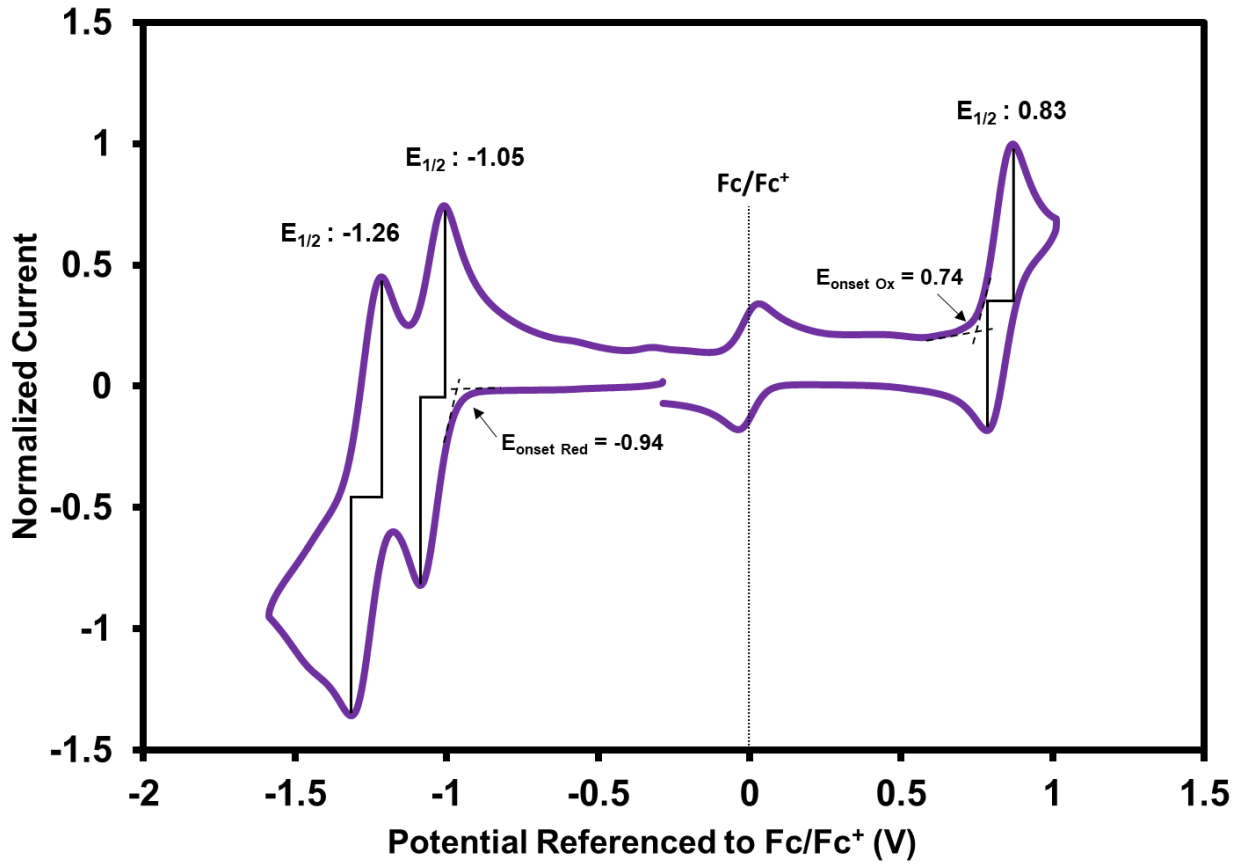

Figure S11. Cyclic Voltammogram of **Br_2-X1** in CH_2Cl_2, recorded at 100 mV/s. Fc/Fc+ couple shown (Fc: ferrocene).

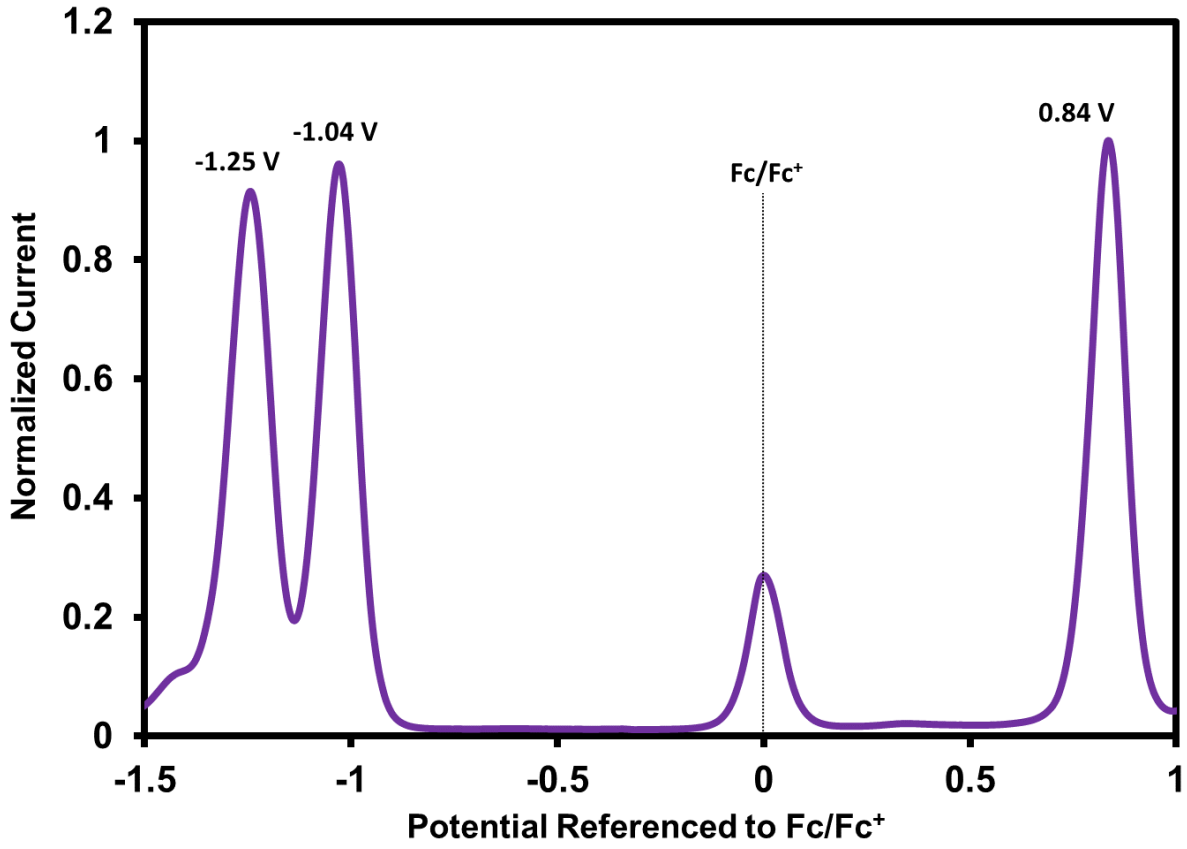

Figure S12. Differential pulse voltammogram of **Br_2-X1** in CH_2Cl_2, recorded at 100 mV/s. Fc/Fc+ couple shown (Fc: ferrocene).

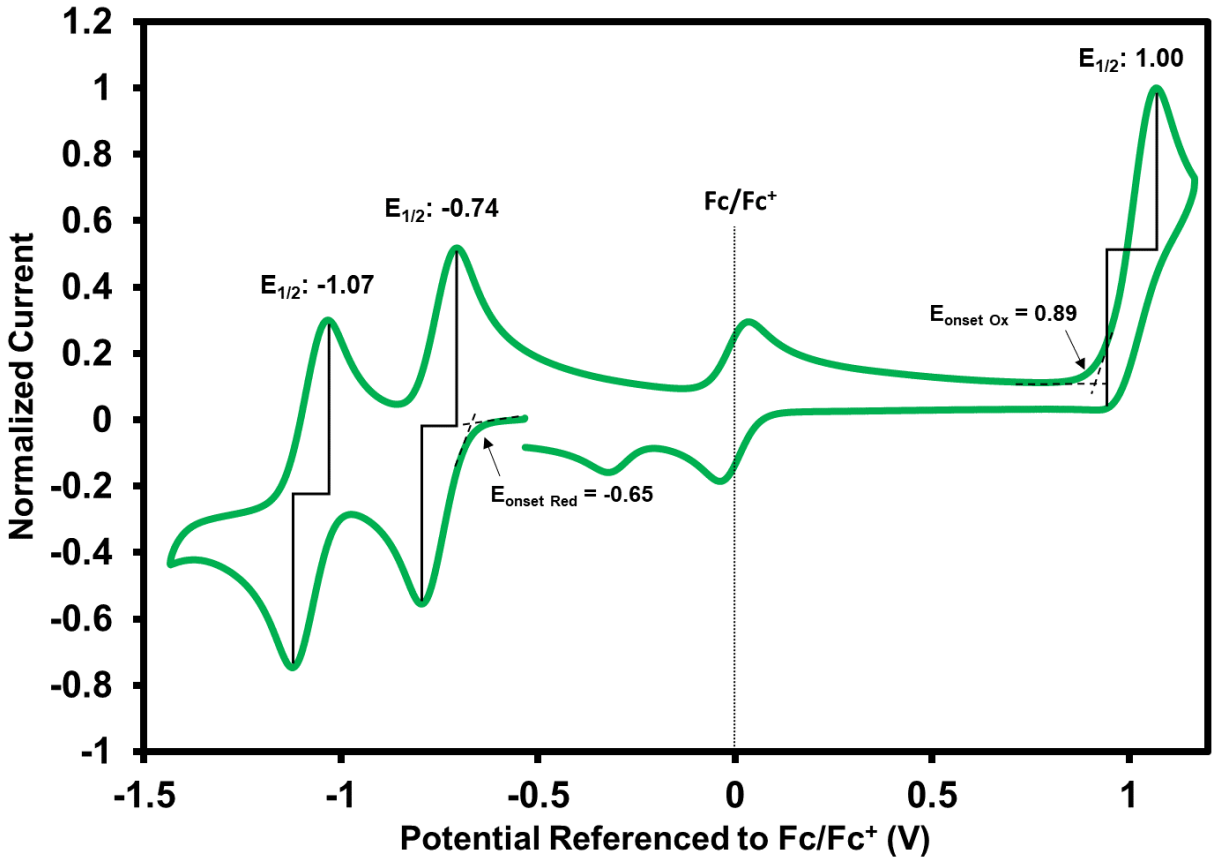

Figure S13. Cyclic Voltammogram of **X6** in CH_2Cl_2, recorded at 100 mV/s. Fc/Fc+ couple shown (Fc: ferrocene).

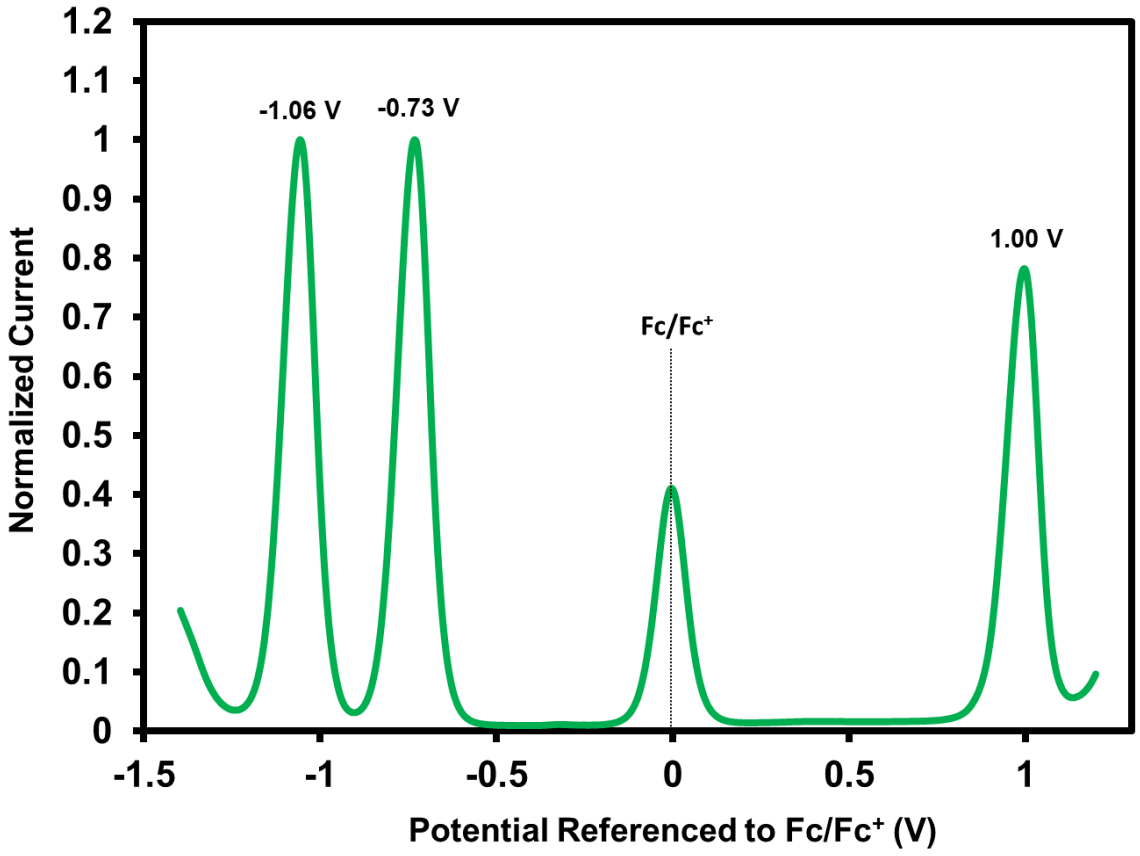

Figure S14. Differential pulse voltammogram of **X6** in CH_2Cl_2, recorded at 100 mV/s. Fc/Fc+ couple shown (Fc: ferrocene).

10. Density Functional Theory (DFT) and pKa Calculation

Compound	State	E_{opt} (eV)	λ (nm)	f	Composition	pKa
X1	S_1	2.0134	615.80	0.3727	H → L (70%)	31.18
	S_2	2.8695	432.08	0.1807	H-1 → L (69%)	
X6	S_1	1.9647	623.01	0.3745	H → L (70%)	26.52
	S_2	2.8051	436.03	0.1505	H-1 → L (67%)	

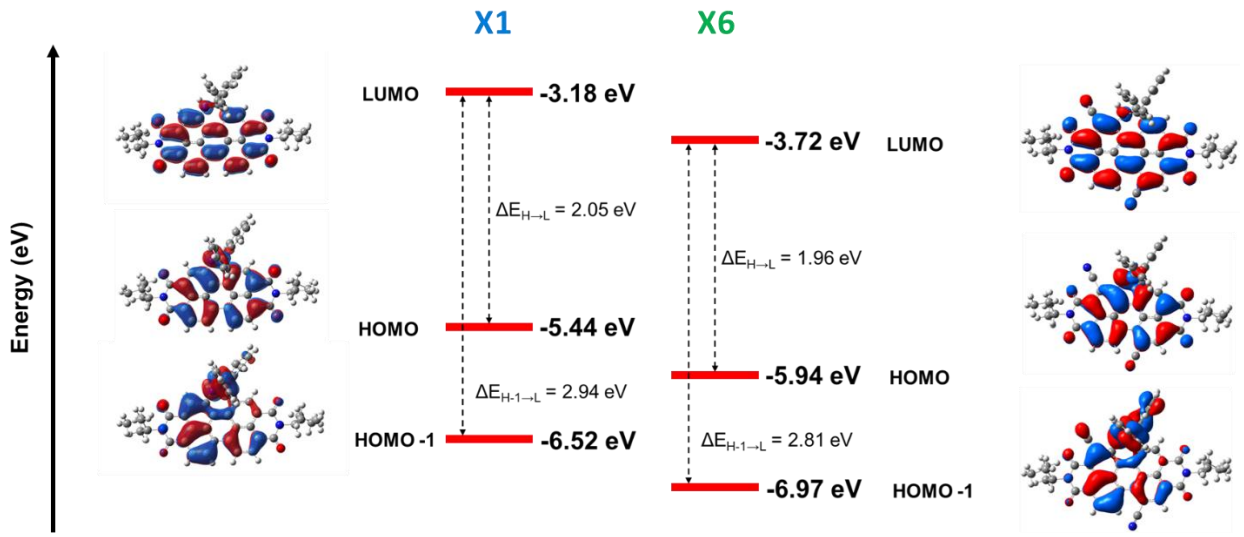

Figure S15. DFT comparison of **X1** and **X6**.

11. X6 Solubility and Film formation

Table S3. X6 solubility in various organic solvents at room temperature

Solvent	Concentration	Solubility
$CHCl_3$	10 mg mL^{-1}	Fully soluble
o-xylene	5 mg mL^{-1}	Fully soluble
Anisole	10 mg mL^{-1}	Fully soluble
2Me-THF	10 mg mL^{-1}	Fully soluble
Toluene	10 mg mL^{-1}	Fully soluble
Ethyl Acetate	1 mg mL^{-1}	Partially soluble

* *o*-xylene (10 mg mL^{-1}) was not fully soluble

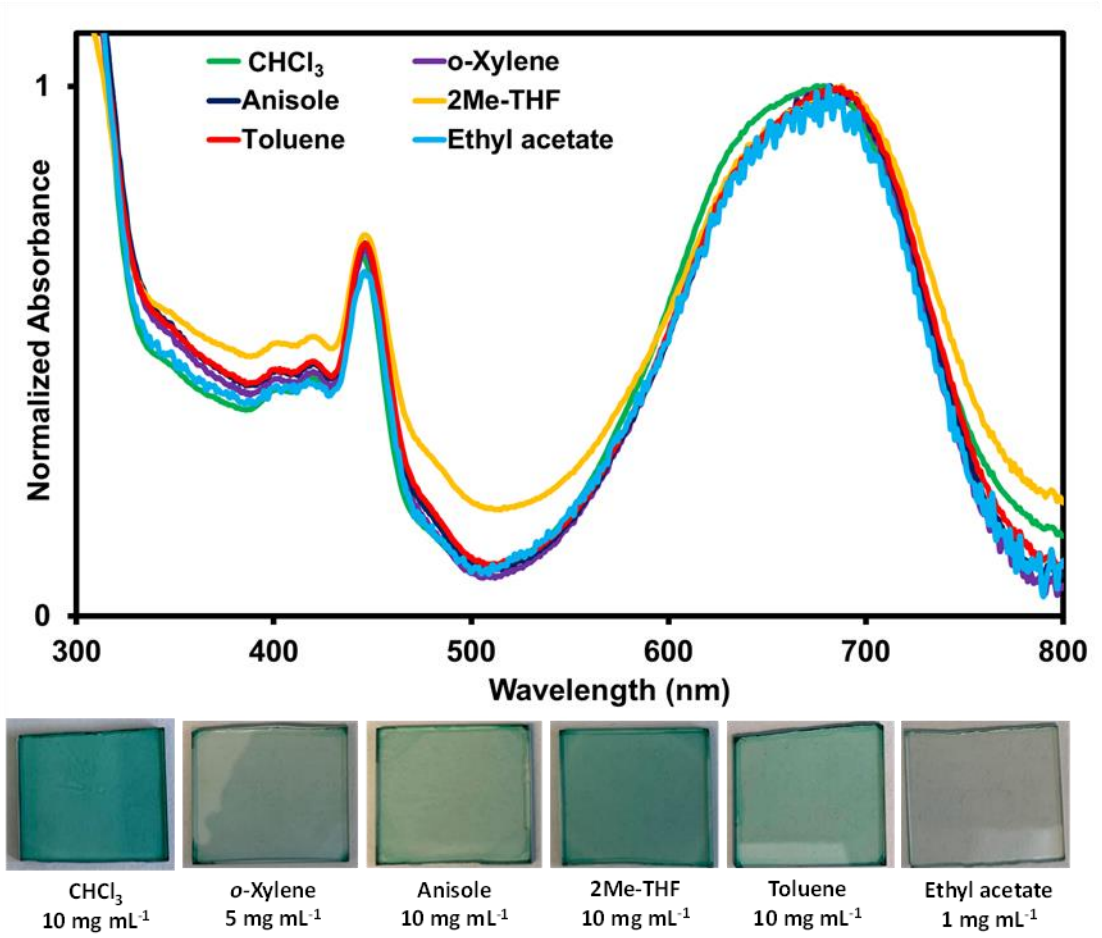

Figure S16. Optical absorption spectra and pictures of spin-casted X6 solutions, 40 μL of each solution is spin-casted on a glass slide at 1000 rpm for 60 seconds.

12. Optical absorption and photoluminescence spectra

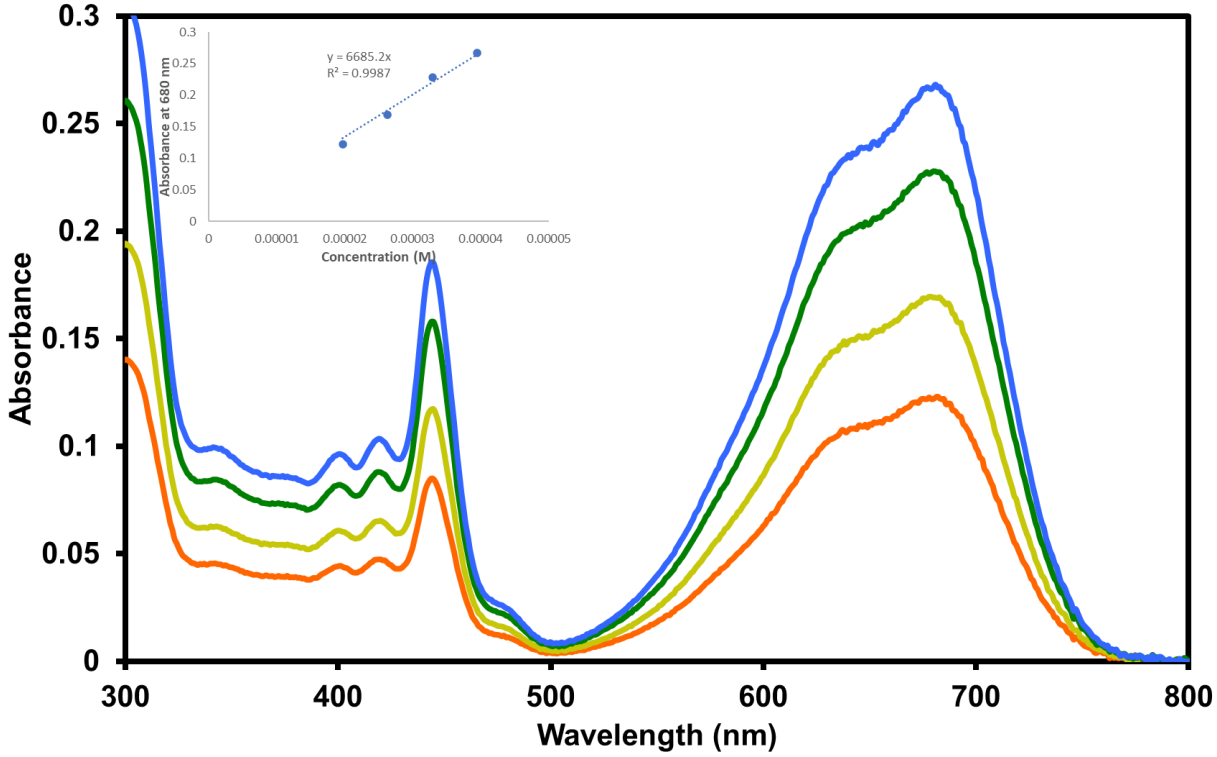

Figure S17. Absorbance calibration curve of **X6** in $CHCl_3$ (ε_{680nm} = 33,426 M^{-1} cm^{-1}).

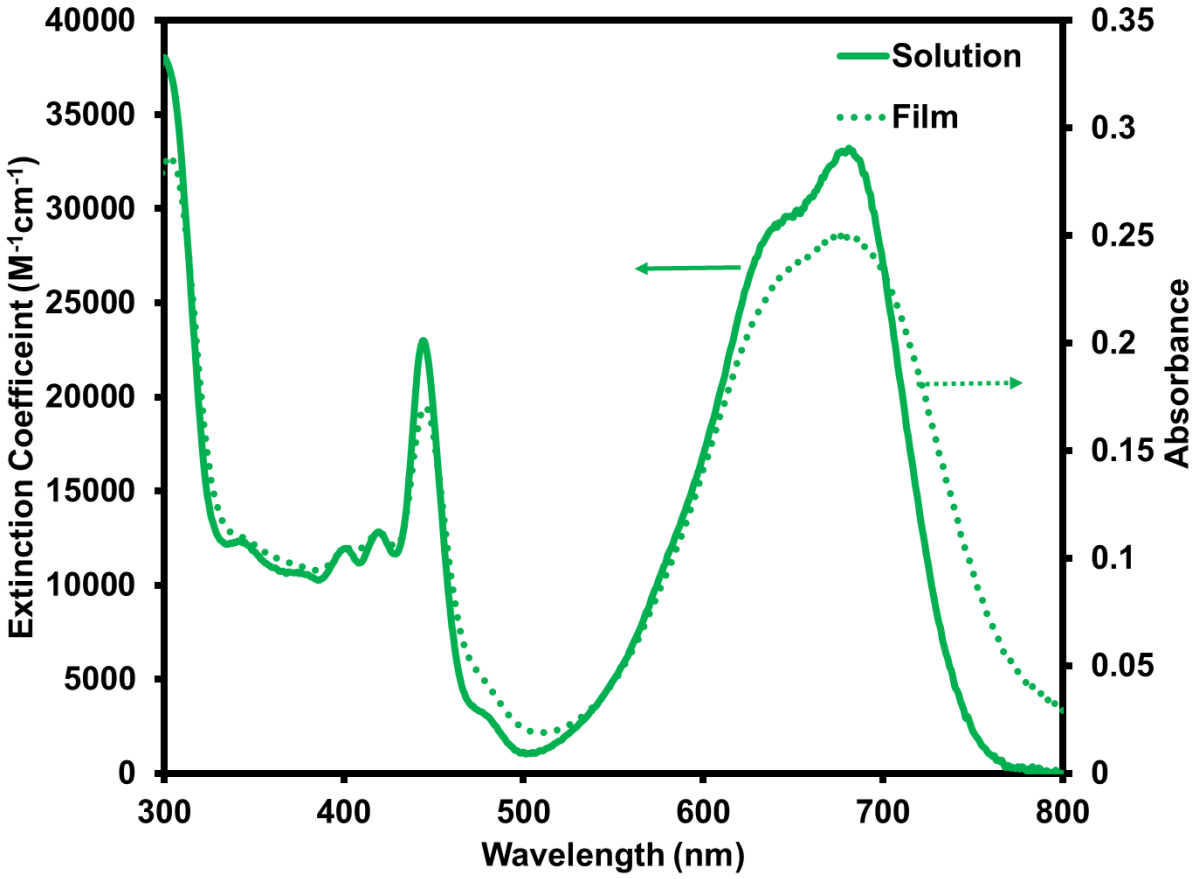

Figure S18. Comparison of the normalized optical absorption spectra of solution ($CHCl_3$) and film (spin-cast from 10 mg/mL in $CHCl_3$) of **X6**.

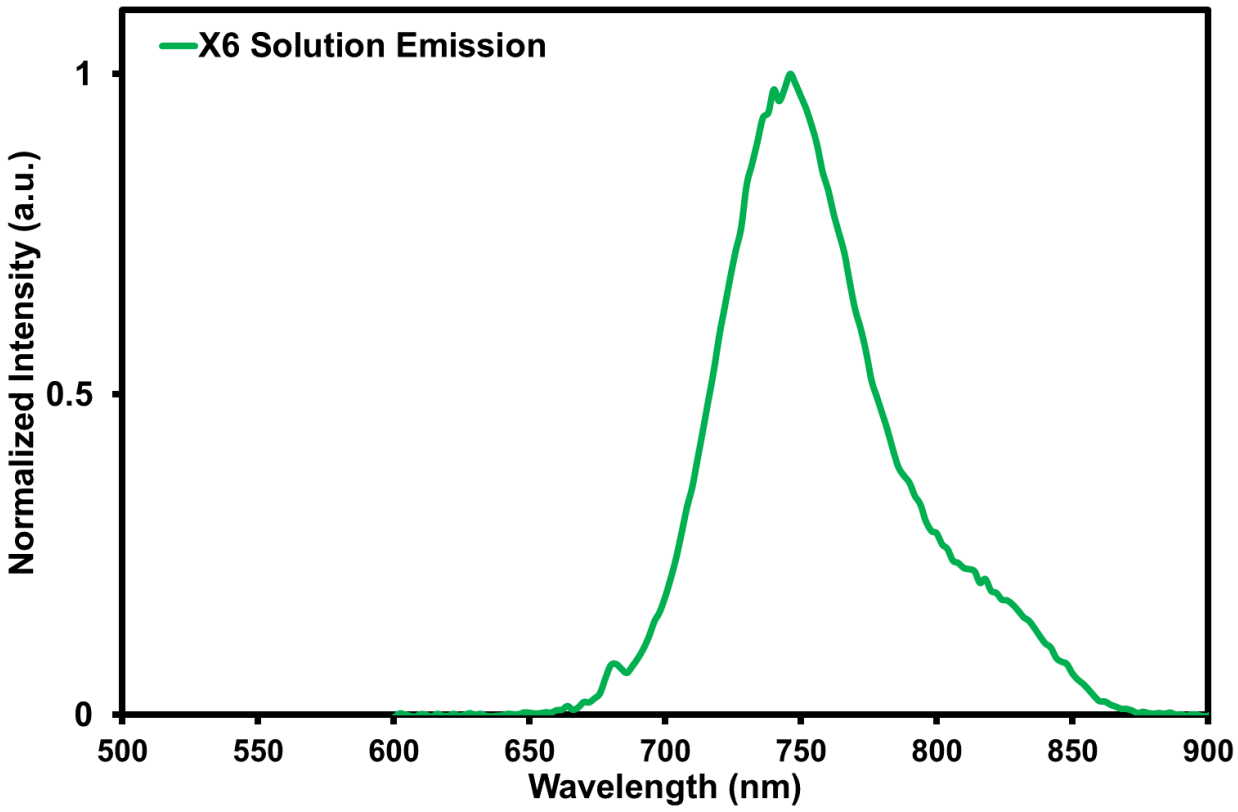

Fig S19. Photoluminescence emission spectra of **X6** in $CHCl_3$ solution. Excitation wavelength = 680nm.

13. OFET Data

Table S4. Electron mobility and threshold voltage of **X6** OFET devices cast from $CHCl_3$ or 2Me-THF and thermally annealed at 70 °C or 150 °C. Averages are presented plus/minus the standard deviation of 4 devices, measurements taken under vacuum (P < 0.1 Pa). Channel width = 2000 µm.

	$CHCl_3$, 70 °C				$CHCl_3$, 150 °C				2Me-THF, 70 °C			
Length (µm)	μ_e ($x10^{-6}$ cm^2/Vs)		V_T (V)		μ_e ($x10^{-6}$ cm^2/Vs)		V_T (V)		μ_e ($x10^{-6}$ cm^2/Vs)		V_T (V)	
20	9.62	±0.82	12.7	±1.4	5.97	±1.14	7.8	±2.4	6.32	±1.76	7.8	±5.1
10	5.01	±2.01	3.8	±4.8	4.71	±0.19	2.5	±0.8	4.97	±0.47	3.8	±1.0
5	7.40	±0.72	2.4	±0.8	6.10	±0.36	0.8	±0.8	8.37	±0.27	2.8	±0.3
2.5	14.4	±0.78	0.7	±0.1	11.3	±0.53	-1.4	±0.4	8.48	±1.40	0.5	±0.4

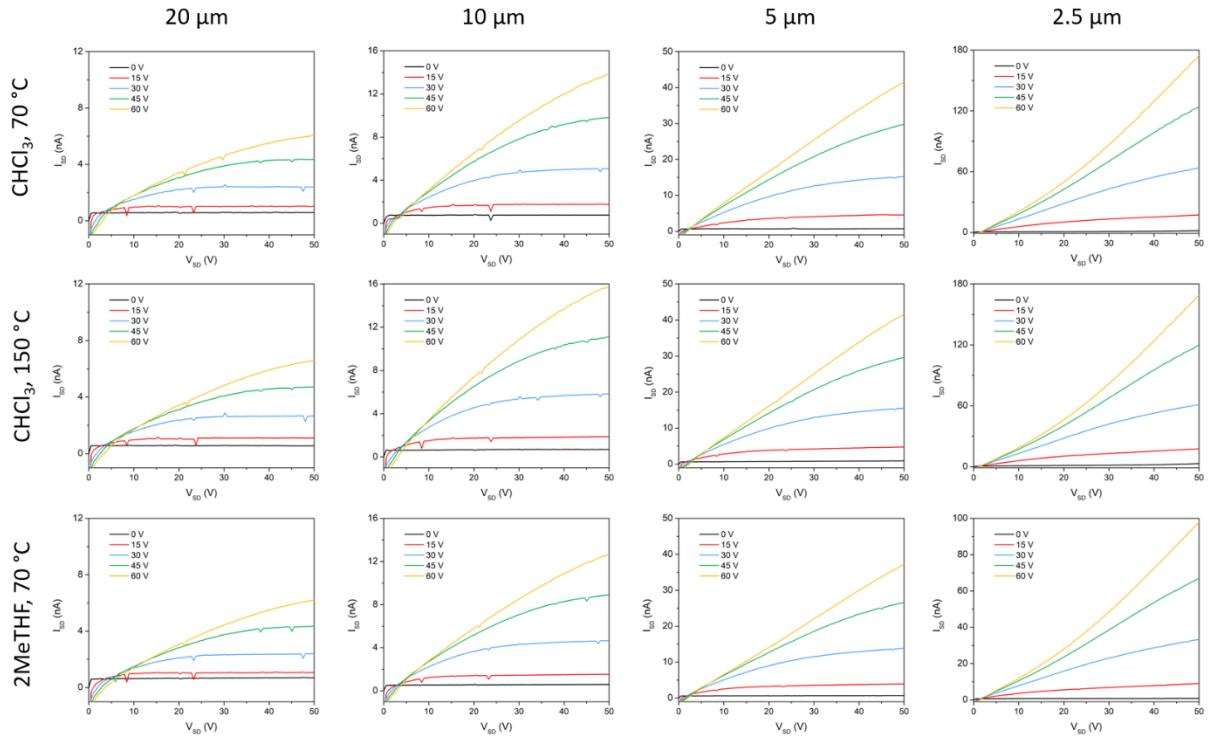

Fig S20. Representative output curve of a 10 µm channel length device from **X6**.

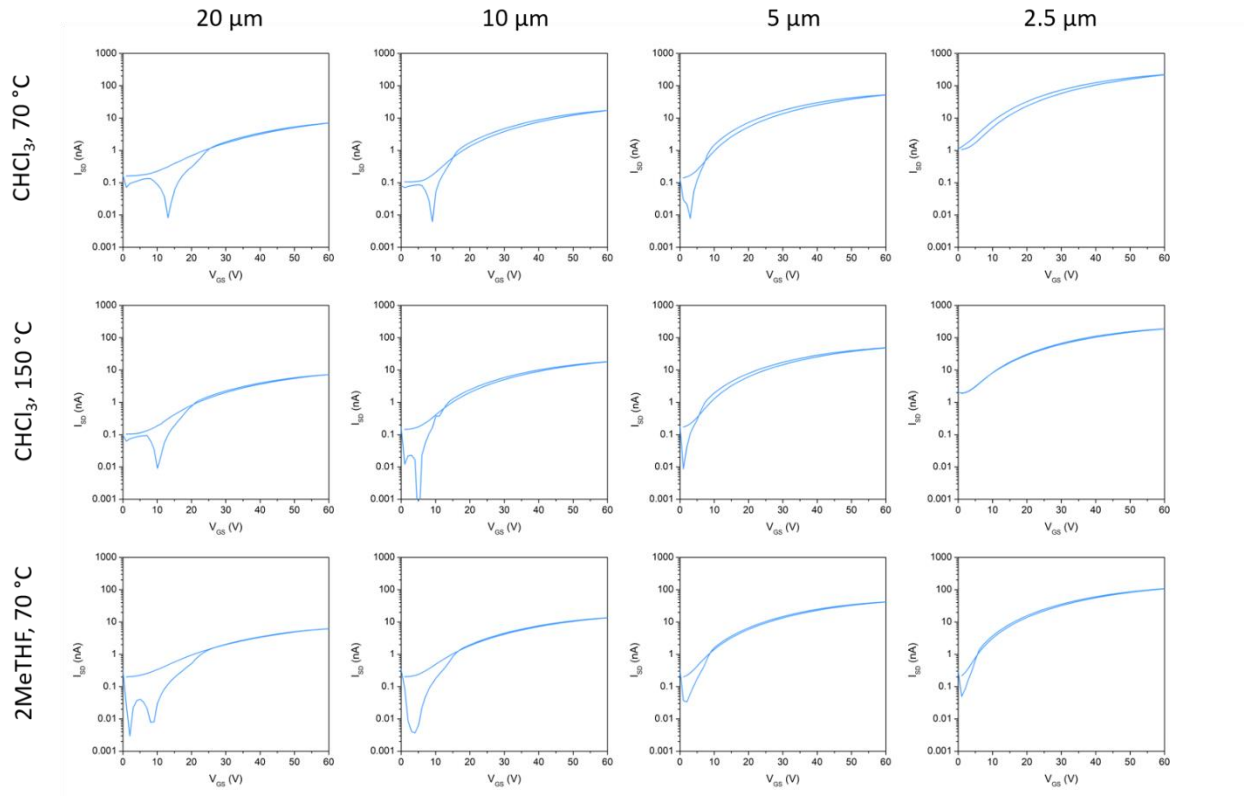

Fig S21. Representative transfer curve of a 10 µm channel length device from **X6**. VSD = 50V.

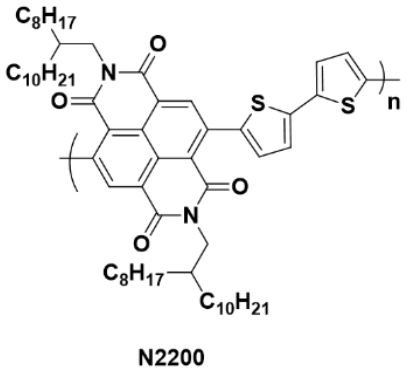

N2200

Fig S22. Chemical structure of the conjugated polymer N2200.

14. References

1. D. H. Harris, S. Brixi, B. S. Gelfand, B. H. Lessard and G. C. Welch, *J. Mater. Chem. C*, 2020, 8, 9811–9815.
2. Bruker-AXS. SAINT; Madison, Wisconsin, USA, 2017.
3. Bruker-AXS. XPREP; Madison, Wisconsin, USA, 2017
4. Dolomanov, O.V., Bourhis, L.J., Gildea, R.J, Howard, J.A.K. & Puschmann, H. (2009), J. Appl. Cryst. 42, 339-341.
5. Sheldrick, G.M. (2015). Acta Cryst. A71, 3-8.
6. Sheldrick, G.M. (2015). Acta Cryst. C71, 3-8.
7. Spek, A.L. (2015). Acta Cryst. C71, 9-18.
8. Frisch, M. J.; Trucks, G. W.; Schlegel, H. B.; Scuseria, G. E.; Robb, M. A.; Cheeseman, J. R.; Scalmani, G.; Barone, V.; Petersson, G. A.; Nakatsuji, H.; et al. Gaussian. Gaussian, Inc.: Wallingford CT 2016.
9. Marenich, A. V.; Cramer, C. J.; Truhlar, D. G. Universal Solvation Model Based on Solute Electron Density and on a Continuum Model of the Solvent Defined by the Bulk Dielectric Constant and Atomic Surface Tensions. *J. Phys. Chem. B* 2009, *113* (18), 6378–6396.
10. Ho, J.; Zwicker, V. E.; Yuen, K. K. Y.; Jolliffe, K. A. Quantum Chemical Prediction of Equilibrium Acidities of Ureas, Deltamides, Squaramides, and Croconamides. *J. Org. Chem.* 2017, *82* (19), 10732–10736.